ELSEVIER

International Journal of Adhesion & Adhesives 26 (2006) 67–78

International Journal of Adhesion & Adhesives

www.elsevier.com/locate/ijadhadh

Factors influencing the durability of epoxy adhesion to silane pretreated aluminium

A.N. Rider*

DSTO, Air Vehicles Division, 506 Lorimer St., Fishermen's Bend, Melbourne 3207, Australia

Available online 5 May 2005

Abstract

Factors that may influence the durability of bonds formed between epoxy adhesive and γ-glycidoxypropyltrimethoxy silane (γ-GPS) pretreated aluminium were investigated. A precision milling apparatus or grit-blasting was used to alter the surface roughness of aluminium adherends prior to adhesive bonding. Addition of γ-GPS to the roughened aluminium surface improved bond durability, but the overall performance was also influenced by the initial surface roughness of the aluminium. The milled ultra-flat aluminium surface exhibited the worst bond durability and the grit-blast and milled surface with a 60° surface profile exhibited the best bond durability. Comparison of the γ-GPS with a range of phosphonate hydration inhibitors also provided information about the influence of interfacial chemical interactions on bond durability. The coupling mechanism between the phosphonate organic ligand and the adhesive influenced bond durability performance. Surface analysis of failed wedge samples, together with characterisation of the structure of the γ-GPS and phosphonate films deposited on aluminium, suggested that the γ-GPS film structure could also affect bond durability performance.

Keywords: B. Aluminium and alloys; B. Surface treatment by chemical solutions; C. X-ray photoelectron spectroscopy; C. Wedge tests

1. Introduction

Work at the Aeronautical and Maritime Research Laboratory (AMRL) by Baker and Chester [1] established that a solvent degrease, followed by a manual abrasion, a grit-blast and an application of γ-glycidoxypropyltrimethoxy silane (γ-GPS) produced a tough, durable bond with selected thermoset epoxy film adhesives. This is now widely known as "The Australian silane surface treatment". Research carried out at AMRL over a number of years [1–7] has examined a range of factors influencing the durability of epoxy bonds formed with aluminium pre-treated using the grit-blast and silane method. The Royal Australian Air Force (RAAF) produced its own Engineering Standard [8] for adhesive bonded repairs due to deficiencies in the manufacturers' Structural Repair Manuals [9]. These steps were taken to improve the credibility of bonded repairs and to assist with their management in the RAAF fleet. The surface preparation principles underpinning this standard were established during the research and development of the Australian silane surface treatment. Kuhbander and Mazza [10] examined the process variables in the grit-blast plus γ-GPS treatment, with the conclusion that the process parameters used by AMRL and RAAF for the treatment were, in general, optimal.

Recently, AMRL has become involved in a collaborative international research programme that was designed to investigate the fundamental nature of interactions between γ-GPS and aluminium [11]. This current paper presents research performed at the Defence Science and Technology Organisation (DSTO) that has examined two aspects of the "Australian silane surface treatment". The first factor examined the influence that surface roughness created by the abrasion and grit-blasting steps had on the performance of the

*Tel.: +61 3 9626 7393; fax: +61 3 9626 7087.
E-mail address: andrew.rider@dsto.defence.gov.au.

0143-7496/$ - see front matter © 2005 Elsevier Ltd. All rights reserved.
doi:10.1016/j.ijadhadh.2005.03.005

γ-GPS treatment. The second factor examined the hydration inhibiting properties of the γ-GPS film in comparison with a class of compounds known as phosphonates. The hydrolytic stability of the interfacial region of the aluminium–epoxy bond is one factor influencing bond durability performance. In some cases, failure of aluminium–epoxy joints has been shown to result from moisture ingress to the interface reacting with the underlying metal substrate and forming a cohesively weak hydrated oxide layer that fails under load [12]. Work by Venables and co-workers [12] indicated that phosphonate hydration inhibitors improved the durability of bonds formed between epoxy adhesive and chromic-acid-etched aluminium by retarding the oxide hydration mechanism. Work examining a number of these phosphonate compounds [5], however, suggested inferior performance relative to the γ-GPS treatment, despite evidence that the phosphonates were as good or better than γ-GPS at inhibiting the hydration of the aluminium oxide surface exposed to high humidity environments.

In this paper, previous work from a larger study investigating factors affecting bond durability is reported [13]. Three novel phosphonate compounds were synthesised. The organic ligand of the phosphonate, which couples to the epoxy adhesive, was modified to more closely resemble the epoxy ligand on the γ-GPS molecule and, thereby, assess the relative importance of this coupling mechanism in the overall bond durability performance of the γ-GPS treatment.

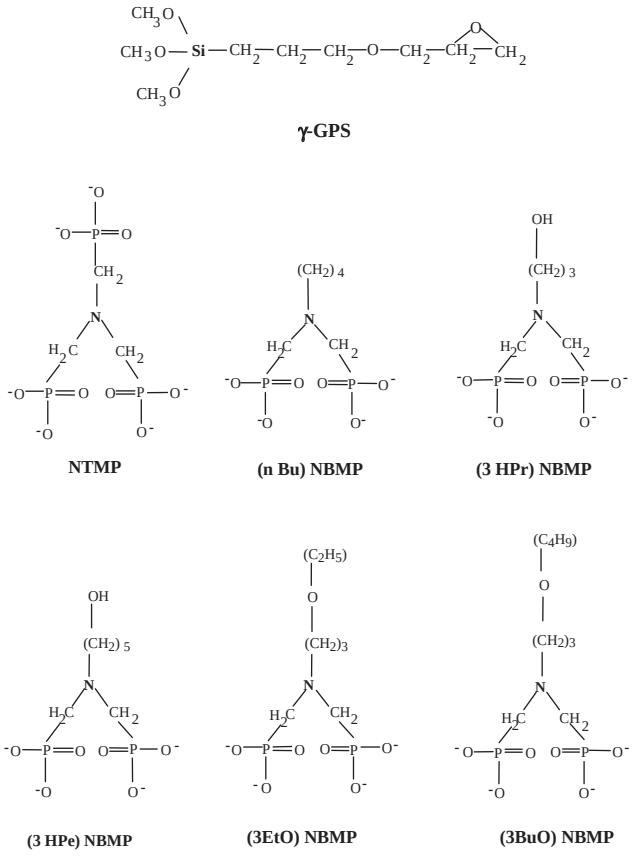

Fig. 1. Chemical structures of the γ-GPS and phosphonate molecules used in the pre-treatment studies.

2. Experimental

2.1. Film characterisation studies

Coupons of Al-2024 T3 clad aluminium alloy were ultramilled, using a precision milling machine to produce flat clean surfaces [14], and dipped in a 1% solution of γ-glycidoxypropyltrimethoxy silane (γ-GPS) (Fig. 1) for 10 min. The 1% solution was prepared using distilled de-ionised water and was stirred for 1 h prior to sample treatment. The natural pH of the γ-GPS solution was 4.5. Upon removal, the sample was rinsed in de-ionised water and dried with a stream of dry nitrogen to remove surface moisture, prior to analysis.

A series of phosphonate hydration inhibitors were also investigated for the purpose of direct comparison with the γ-GPS. The inhibitors investigated have their chemical structures and abbreviated names displayed in Fig. 1 and Table 1, respectively. The first three compounds in Table 1 were obtained commercially. The remaining three phosphonates were synthesised by reacting an alkoxypropyl amine with formaldehyde and phosphoric acid in the molar ratio of 1:3.5:2 [15]. The compound purity was assessed with melting point measurements. Ultramilled Al-2024 T3 clad aluminium was immersed in 100 ppm phosphonate solutions for 15 min. The solution of phosphonate was adjusted to a pH of 3.5 with dilute HNO_3 or NaOH additions. Samples were thoroughly rinsed after removal from solution and dried.

X-ray photoelectron spectroscopy (XPS) was performed using a Kratos model XSAM-800 spectrometer. MgK_α radiation illuminated the surface with a power of 30 W. Film characterisation studies used fixed analyser transmission (FAT) mode with a pass energy of 20 eV and quantification was performed using sensitivity factors derived using reference compounds which included $AlPO_4$, Al_2O_3, poly(dimethylsiloxane) (PDMS) and SiO_2 (quartz). All spectra were calibrated relative to the C1s line from saturated hydrocarbon (CH_n) at 285.0 eV.

Reflection–absorption infrared (RAIR) spectra were collected using a grazing angle bench that enabled the beam to be focussed on the sample at 80° relative to the surface normal. The reflected beam was recorded with a 4 cm^{-1} resolution and averaged over 256 scans. An untreated, ultramilled aluminium specimen was used to acquire the background spectrum. The reaction of the γ-GPS in solution, prior to sample immersion, was also

Table 1
List of abbreviated titles used to describe the phosphonates studied

Phosphonate	Abbreviation
Nitrilotris methylene phosphonic acid	NTMP
n Butyl nitrilobis methylene phosphonic acid	(n Bu) NBMP
3-hydroxypropyl nitrilobis methylene phosphonic acid	(3HPr) NBMP
3-hydroxypentyl nitrilobis methylene phosphonic acid	(3HPe) NBMP
3-ethoxypropyl nitrilobis methylene phosphonic acid	(3EtO) NBMP
3-butoxypropyl nitrilobis methylene phosphonic acid	(3BuO) NBMP

studied using Fourier transform infrared (FT-IR). Small volumes of a 3% γ-GPS solution were analysed at different times using a recess mounted ZnSe crystal trough assembly. This unit enabled six reflections at a 45° incident angle. The spectra acquired were averaged over 200 scans and the γ-GPS spectrum was obtained by subtracting the water spectrum from the 3% γ-GPS spectrum.

2.2. Bond durability and fracture studies

Al-2024 T3 clad aluminium adherends of 3.15 mm thickness were used for fabrication of wedge specimens, prepared in accordance with ASTM D3762-79 [16]. The thicknesses of the wedges driven into the bonded joints, in order to force fracture, were 1.6 and 3.2 mm for the surface roughness and phosphonate studies, respectively. Thinner wedges were required for the surface roughness studies as the 180° ultramilled surfaces performed so poorly that the standard wedge thickness caused complete specimen failure. FM-73© epoxy structural adhesive from Cytec-Fiberite was used for all wedge specimens. The ultramilled aluminium plates were bonded at 120 °C and 275 kPa in a platen press for 1 h. The initial crack lengths of the wedge specimens were allowed to equilibrate for several hours at ambient, which was typically 20 °C and 50% relative humidity (R.H.), prior to transfer to an isothermal enclosure that was adjusted to 50 °C and 95% R.H. Crack growth measurements were made on a periodic basis over approximately 200 h. XPS analysis was performed on the surfaces of the failed specimens as close as possible to the crack tip region using a fixed retard ratio (FRR) of 53 and high magnification, where the area of analysis was approximately 2 mm in diameter. FRR is the only mode of operation offered by the spectrometer that provides small area analysis capability. The sensitivity factors provided by the manufacturer for the FRR mode of operation were used to quantify the data.

Roughness studies involved either ultramilling [14] or grit-blasting aluminium adherends prior to treatment.

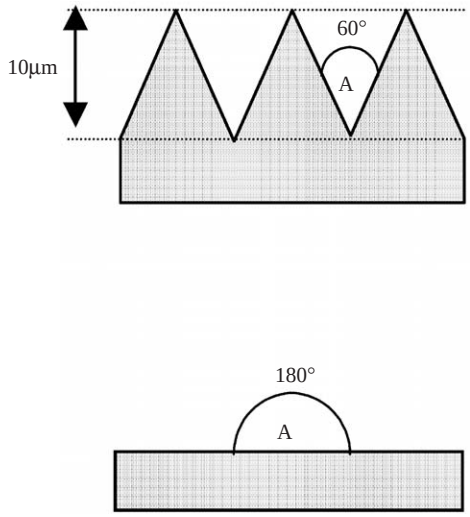

Fig. 2. Diagrammatic cross-sections indicating the profile angle, A, for the ultra-flat 180° and rough 60° ultramilled Al-2024 T3 clad aluminium surfaces.

The ultramilling process was conducted with specially manufactured milling blades to produce three sawtooth profiles of 180°, 120° and 60°. The rough, 60°, and flat, 180°, profiles are described diagrammatically in Fig. 2. The 40 mm milling radius produced a groove direction perpendicular to the sample length. The automated grit-blast treatment was conducted using 50 μm alumina particles delivered with an impact density of 1.2 g cm^{-2} [17]. Ultramilled samples were treated with γ-GPS using the conditions described in Section 2.1.

AFM images of 180° ultramilled and grit-blasted aluminium have been shown previously [14]. Statistical analysis of the 180° ultramilled AFM images indicated that over areas of 3600 μm^2, which included flat regions and grooves, there was a root mean square surface roughness (R_{rms}) of 12 ± 2 nm and an average roughness (R_{av}) of 7 ± 2 nm. In areas of 100 μm^2, between the grooves, the R_{rms} was 1.4 ± 0.2 nm and the R_{av} was 0.9 ± 0.1 nm. The relative surface area was 1.0. In the case of the grit-blasted surface for areas of 3600 μm^2, the peak to valley roughness (R_{p-v}) was 2.4 ± 0.4 μm with a R_{rms} of 0.52 ± 0.05 μm and a R_{av} and relative surface area of 0.41 ± 0.03 μm and 1.35 ± 0.10, respectively.

The relative durability performance of the phosphonate and γ-GPS chemicals was compared by pretreating adherends of Al-2024 T3 clad aluminium alloy samples for 15 min in a 65 °C chromic acid etch (CAE) solution, followed by tap and de-ionised water rinsing. The CAE solution had the following composition (g dm^{-3}): $Na_2Cr_2O_7.2H_2O$ (60), H_2SO_4 (318), Al-2024 T3 aluminium (1.3), de-ionised water (balance) [18]. The CAE-prepared plates were treated with the phosphonates listed in Table 1, or the γ-GPS and bonded with FM-73 adhesive in an autoclave at 275 kPa and 120 °C for 60 min. Bond durability tests were carried out in the

Table 2
Atomic composition for γ-GPS and phosphonate-treated 180° ultramilled aluminium

Treatment	Element/atomic concentration (%)									
	Al2p		Si2s	P2s	C1s				N1s	O1s
	Oxide	Metal			285 eV	286.0–286.5 eV	288.4 eV	289.4 eV		
Ultramilled	24.0	22.1	—	—	5.9	1.4	0.4	1.0	—	45.2
γ-GPS	16.3	15.7	3.3	—	8.3	10.1	1.5	0.3	—	44.5
NTMP	20.3	12.0	—	4.8	6.6	4.1	0.6	0.4	1.6	49.6
(nBu) NBMP	21.7	14.5	—	3.2	7.1	3.4	0.3	0.5	1.1	48.2
(3HPr) NBMP	22.7	15.2	—	2.9	5.4	2.8	0.3	0.4	1.2	49.1
(3HPe) NBMP	21.2	12.4	—	4.0	8.8	3.4	0.7	0.2	1.4	47.9
(3EtO) NBMP	20.1	14.6	—	3.8	8.0	3.5	0.5	0.5	1.6	47.4
(3BuO) NBMP	20.6	12.6	—	3.7	8.9	5.2	0.5	0.4	1.4	46.8

condensing humidity above a water bath maintained at 50 °C. The condensing humidity environment contrasts with the non-condensing 95% R.H. environment used for the roughness studies.

The relative bond durability performance was compared to the standard phosphoric acid anodise (PAA) treatment [18] used by the aerospace industry for adhesively bonding to aluminium. Briefly, this procedure involves treating the aluminium using the CAE process, followed by anodisation in a 10% aqueous solution of phosphoric acid at 10 V for 25 min, followed by tap and de-ionised water rinsing.

3. Results

3.1. Film characterisation

The atomic compositions of the ultramilled Al-2024 T3 clad aluminium before and after treatment with a 1% aqueous γ-GPS and 100 ppm phosphonate solutions are shown in Table 2. Peak fitting of the C1s spectra (Fig. 3) used four components [19] and their relative percentages are provided in Table 2. Three of the four components are clearly resolvable at 285, 286.5 and 289.4 eV. The remaining peak at 288.4 eV is attributed to a carbonyl vibration. This peak is justified on the basis of previous work that examined the pre-treatment of aluminium [20]. XPS spectra taken on aluminium after methyl ethyl ketone cleaning (MEK) showed a notable increase in this region of the C1s spectrum and after grit-blasting the aluminium, in which the MEK was removed from the surface, the intensity at 288.4 eV reduced to almost zero. The elemental ratios of the γ-GPS and phosphonate films were calculated and are provided in Table 3, together with the expected ratio, based on the molecular structure. The stoichiometric ratios calculated in Table 3 assumed an O to Al ratio of 1.8, determined from the ultramilled sample, and allowed for contributions to the O1s peak from the high-binding-energy C1s peaks fitted at 288.4 and 289.4 eV.

Angle-resolved XPS (ARXPS) experiments were conducted on ultramilled aluminium treated with γ-GPS and phosphonate solutions. Eq. (1) was employed to calculate the film thickness and surface coverage [21]:

$$\frac{I_{\mathrm{C1s}}}{I_{\mathrm{Al2p}}} = \frac{Cf_{\mathrm{p}}(1-R)}{(1-f_{\mathrm{p}})+f_{\mathrm{p}}R}, \tag{1}$$

where

$$R = 1 - \exp\left(-T_{\mathrm{C}}/\lambda_{\mathrm{CC}}\,\sin(\theta)\right) \tag{2}$$

and

$$C = \left(\frac{n_{\mathrm{C}}}{n_{\mathrm{Al}}}\right)\left(\frac{\mathrm{KE_C}}{\mathrm{KE_{Al}}}\right)\left(\frac{\Omega_{\mathrm{C}}}{\Omega_{\mathrm{Al}}}\right)\left(\frac{\lambda_{\mathrm{CC}}}{\lambda_{\mathrm{AC}}}\right). \tag{3}$$

I_{C1s} is the intensity of the C1s signal from the carbon overlayer at the specific photoelectron take-off angle, θ, I_{Al2p} is the intensity of the Al2p signal from the substrate, T_{C} is the thickness of the carbon layer with a fractional coverage of f_{p} and λ_{CC} and λ_{AC} are the attenuation lengths of the C1s photoelectron and the Al2p photoelectron in the carbon overlayer, respectively. The values of λ_{CC} and λ_{AC} used were 3.0 and 2.6 nm, respectively [22]. The remaining terms in Eq. (3) refer to the atomic density in the carbon or aluminium layer, n_{C} and n_{Al}, the kinetic energy of the C1s and Al2p lines, $\mathrm{KE_C}$ and $\mathrm{KE_{Al2p}}$, and their respective photoelectric cross-sections, Ω_{C} and Ω_{A12p}.

The results for the γ-GPS and the phosphonate treatments in Fig. 4 indicate that the surface coverage is between 95% and 100% for most treatments with the γ-GPS exhibiting the thickest layer.

Fig. 5 shows the FT-IR spectra taken over 90 min for a 3% γ-GPS aqueous solution. The 3% solution concentration used for the solution studies was the minimum concentration that could be accurately detected using the ATR accessory. The peaks of interest are those at 1197 and 1061 $\mathrm{cm^{-1}}$, due to the $\mathrm{SiOCH_3}$

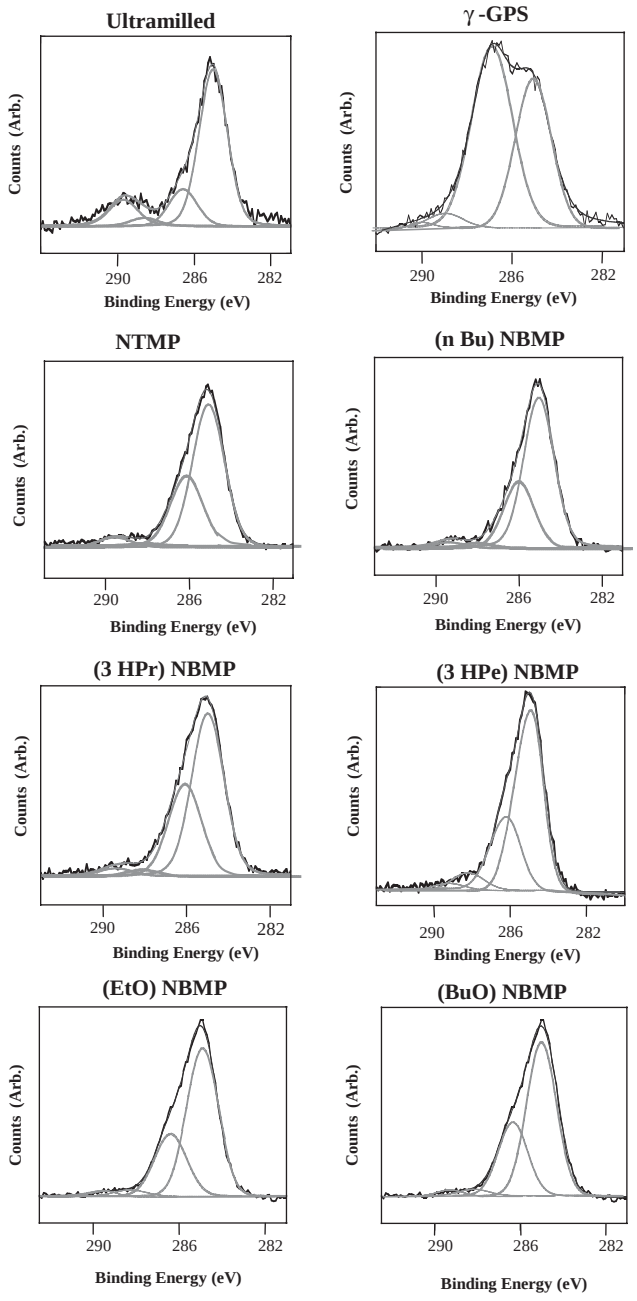

Fig. 3. Peak fitting of the C1s photoelectron spectra from 180° ultramilled Al-2024 T3 clad aluminium surfaces treated with γ-GPS or phosphonate hydration inhibitors.

bond, 1017 cm^{-1}, due to methanol, and 914 and 845 cm^{-1} due to the SiOH bond [23,24]. The peak at 1096 cm^{-1} has a contribution from the $SiCH_2R$ backbone of the organo-silane molecule. The results indicate that with time the methoxy groups are hydrolysed and silanol groups are formed. Hydrolysis has begun to take place within the first 15 min with few methoxy groups present in the 90 min spectrum. There is no evidence of peaks due to the condensation reaction of the silanol groups, which will result in the production of siloxane, Si–O–Si, bonds.

Table 3
Elemental ratio calculated for γ-GPS and phosphonate films deposited on 180° ultramilled aluminium

Treatment	Elemental ratio	Photoelectron line				
		Si2s	C1s	O1s	P2s	N2s
γ-GPS	Theory	1	6	5	—	—
	Measured	1	6.2	4.0	—	—
NTMP	Theory	—	3	9	3	1
	Measured	—	7.3	7.3	3.0	1.0
(nBu) NBMP	Theory	—	6	6	2	1
	Measured	—	7.0	5.0	2.0	0.7
(3HPr) NBMP	Theory	—	5	7	2	1
	Measured	—	6.2	4.8	2.0	0.8
(3HPe) NBMP	Theory	—	7	7	2	1
	Measured	—	6.6	4.4	2.0	0.8
(3EtO) NBMP	Theory	—	7	7	2	1
	Measured	—	6.6	5.2	2.0	0.8
(3BuO) NBMP	Theory	—	9	7	2	1
	Measured	—	8.2	4.4	2.0	0.8

Fig. 6 shows the RAIR spectrum acquired for the film deposited on Al-2024 clad aluminium from 1% γ-GPS aqueous solution. The spectrum in the region between 700 and 1300 cm^{-1} is similar to that reported by Underhill et al. [24,25] for 1% aqueous solutions of γ-GPS deposited on CAE-etched aluminium. The spectrum indicates a broad shoulder on the large peak centred at 1101 cm^{-1}. Whilst the peaks cannot be resolved in this region, Underhill et al. [24] suggests that they are due to the Si–O–Si asymmetric stretch, as do previous workers [26–28], who have used surface-sensitive infra-red techniques to study silane films deposited on metal surfaces. Notably, the peaks near 914 and 845 cm^{-1}, seen in the solution studies due to silanol group vibrations, are not present. The absence of silanol groups appears to be consistent with the small absorbance at 3226 cm^{-1} where the hydroxyl stretching mode is observed. Underhill et al. [24] observed a peak at 1133 cm^{-1}, which was attributed to a cross-linking reaction between the silanol and epoxy groups on neighbouring molecules. The spectrum in Fig. 6 does not appear to indicate an absorbance at this wavenumber, although the spectral resolution in this work is inferior. The peak at 905 cm^{-1} has been attributed to the epoxy group in the γ-GPS molecule [25], whereas the peak at 855 cm^{-1} may be associated with a Si–O–Si vibrational mode [24], possibly providing additional evidence of the presence of siloxane formation in the γ-GPS film.

3.2. Adhesion durability and failure surface analysis

Fig. 7 shows crack-length as a function of exposure time to 50 °C/95% R.H. for ultramilled aluminium

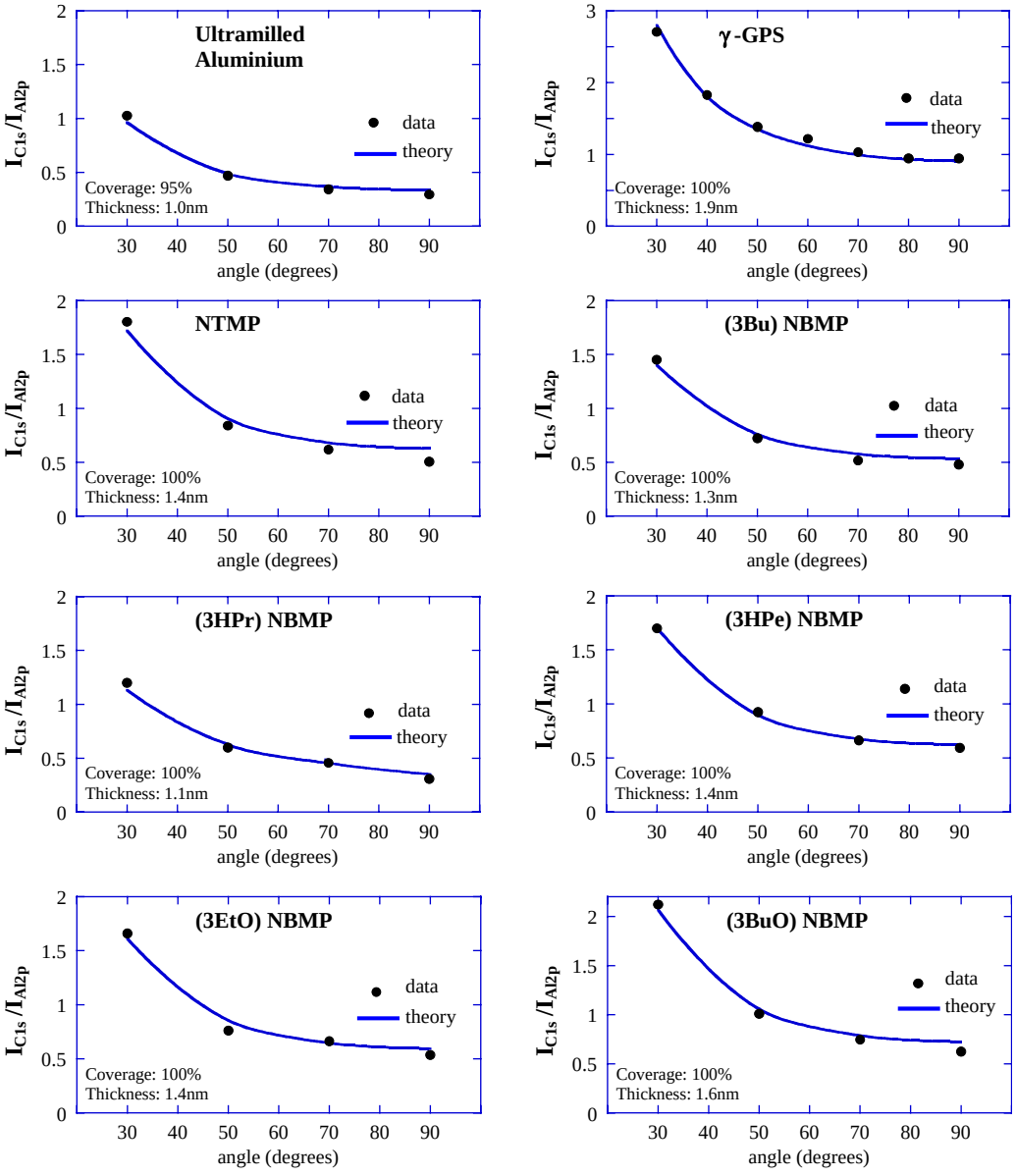

Fig. 4. Angle-resolved XPS measurements of 180° ultramilled Al-2024T3 clad aluminium treated with γ-GPS or phosphonate hydration inhibitors, indicating the data fit used to calculate film thickness and coverage.

before and after treatment with γ-GPS. The untreated aluminium (Fig. 7a) indicates that the durability performance decreases as the surface roughness decreases. The addition of the γ-GPS to the ultramilled and grit-blasted surfaces (Fig. 7b) improves the durability performance; however, there is still an indication that the overall durability performance of the γ-GPS treatment is influenced by the initial surface topography of the aluminium adherend.

Results from the XPS analysis of the failure surfaces produced in the wedge durability experiments are displayed in Table 4. The data in Table 4 suggest that failure occurs near the interface between the adhesive and the metal for the ultramilled samples. In the case of the grit-blast treatment, the failure appears to be interfacial with some evidence of failure within an hydrated oxide layer, as suggested by the aluminium signal on the adhesive fracture face. Interpretation of this failure mode is not straightforward. Investigations by other researchers [29] have indicated that aluminium surfaces exposed in the humid test environment after bond fracture may produce aluminium hydroxide. The aluminium hydroxide possibly dissolves in the humid environment and may redeposit on the adhesive surface, therefore masking the true failure mechanism.

The γ-GPS-treated aluminium samples (Table 4) indicate that the 180° profile has predominantly interfacial failure near the γ-GPS layer. The 120° sample

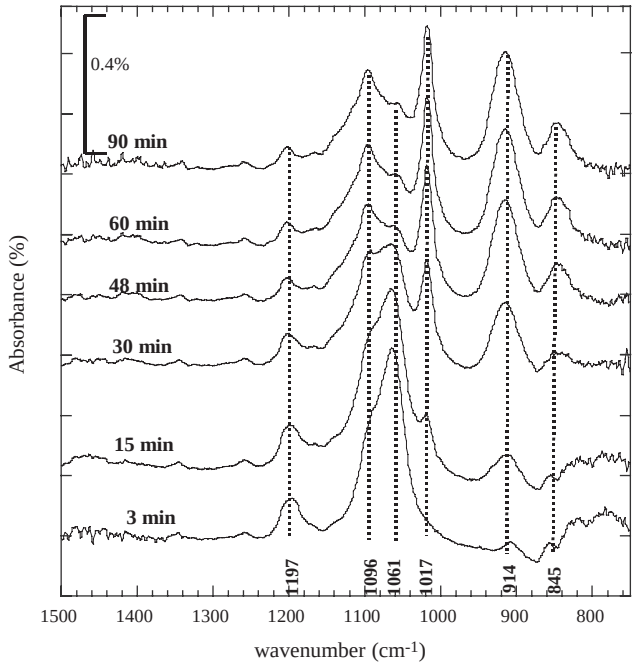

Fig. 5. Infrared spectra of 3% γ-GPS solutions as a function of hydrolysis time in de-ionised water.

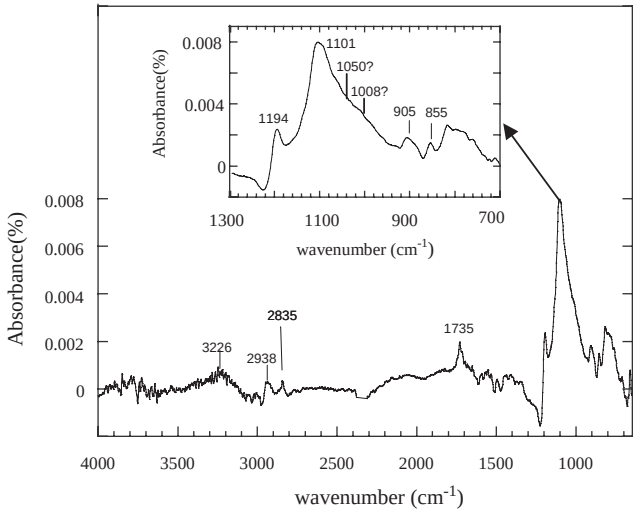

Fig. 6. Reflection–absorption infrared spectrum of ultramilled Al-2024 T3 clad aluminium treated with a 1% aqueous solution of γ-GPS.

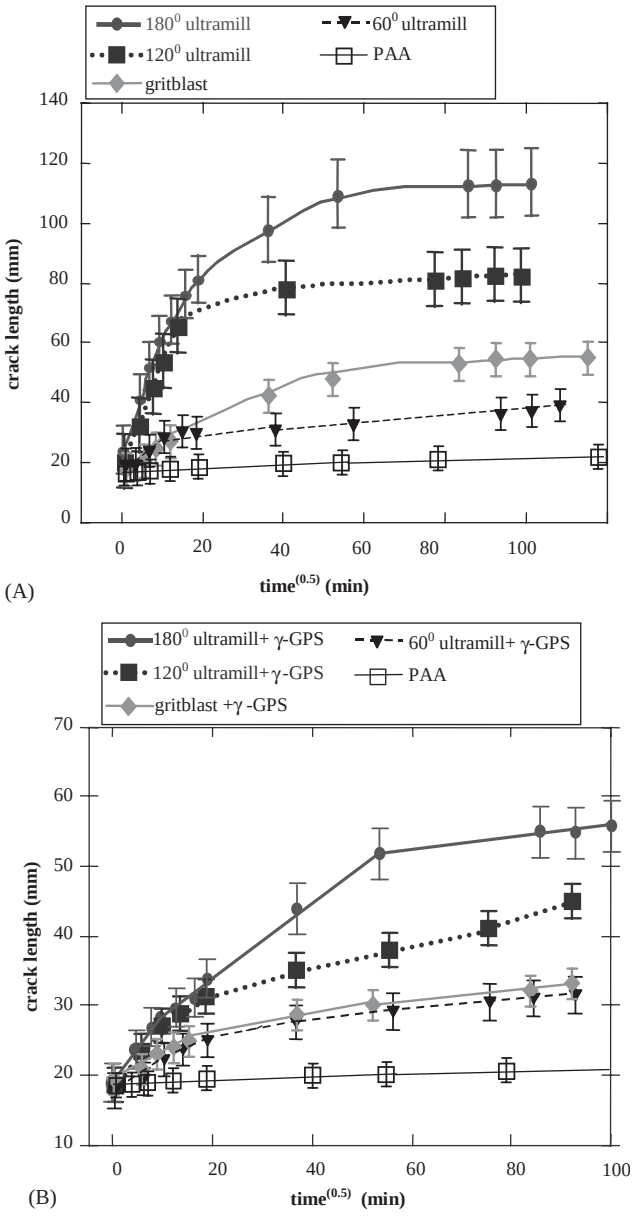

Fig. 7. Wedge test data indicating the durability of Al-2024 T3 clad aluminium (A) ultramilled or grit-blasted and (B) ultramilled or grit-blasted and treated with 1% γ-GPS prior to bonding with FM-73 adhesive.

indicates aluminium on both failure surfaces, suggesting some failure through a weakened oxide layer; however, the presence of silicon on the adhesive surface also suggests that some fracture may have propagated near the γ-GPS layer. The 60° profile sample shows the presence of silicon on both fracture faces and a low aluminium concentration on the adhesive face. This suggests that the fracture path occurs near the adhesive and γ-GPS interface. Some evidence for crack propagation near the epoxy layer is also provided by the nitrogen, from the adhesive, detected on both fracture surfaces. The grit-blast and γ-GPS-treated sample shows the presence of aluminium on the adhesive face, which may suggest that some failure occurs within a weak hydrated oxide layer. Silicon on the adhesive fracture surface possibly indicates that some fracture also occurs near the γ-GPS layer. The presence of aluminium on the adhesive face is similar to the grit-blast treatment and should also be considered in terms of possible changes in the fracture surface composition that may have occurred post-fracture [29]. None of the treatments approach the level of durability observed for the PAA treatment. Visual observation of the failed PAA sample

Table 4
Failure surface composition of ultramilled and grit-blasted aluminium wedge test specimens, before and after γ-GPS treatment

Pre-treatment	Failure surface	Atomic composition (%)				
		O1s	N1s	C1s	Al2p	Si2s
180° ultramilled	Metal	46.4	—	28.7	24.9	—
	Adhesive	25.7	0.8	69.7	3.8	—
120° ultramilled	Metal	52.6	0.3	21.5	25.6	—
	Adhesive	19.3	2.4	76.2	2.1	—
60° ultramilled	Metal	48.4	1.3	26.0	24.3	—
	Adhesive	12.3	1.8	85.3	0.6	—
Grit-blast	Metal	49.5	—	25.9	24.6	—
	Adhesive	19.2	1.9	69.9	9.0	—
180° ultramilled +γ-GPS	Metal	48.1	—	17.4	33.3	1.2
	Adhesive	18.9	1.2	75.2	3.1	1.6
120° ultramilled +γ-GPS	Metal	46.4	—	24.8	28.8	—
	Adhesive	38.3	—	44.3	16.9	0.5
60° ultramilled +γ-GPS	Metal	33.3	1.0	46.1	18.1	1.5
	Adhesive	14.5	1.3	83.1	0.7	0.4
grit-blast +γ-GPS	Metal	48.4	—	19.4	32.2	—
	Adhesive	28.0	0.7	58.9	12.0	0.4

revealed that fracture occurred within the epoxy adhesive layer.

The durability data for CAE-treated aluminium immersed in either 1% γ-GPS solution or the 100 ppm solutions of the phosphonates (Table 1) is shown in Fig. 8(a) and (b). The data in Fig. 8(a) indicate that the γ-GPS treatment improves the durability of the CAE-treated surface. The phosphonate molecules with a hydrocarbon chain or hydrocarbon chain with a hydroxyl end group either perform worse or at a similar level to the untreated CAE surface. Fig. 8(b) shows that the basic NTMP phosphonate or the phosphonates with a butoxy or ethoxy end group improve the durability of the CAE treatment but not to the same extent that the γ-GPS treatment does. No wedge test samples displayed the bond durability performance of the PAA treatment, which indicated minimal crack growth and cohesive fracture of the adhesive.

The fracture analyses of the CAE surfaces treated with γ-GPS and phosphonate are indicated in Table 5. The samples all display the presence of phosphorous or silicon on both surfaces of the failed bond specimen. Low concentrations of aluminium on the adhesive failure surface suggest that the failure is predominantly near the γ-GPS or phosphonate layer.

4. Discussion

4.1. Film characterisation

The FT-IR solution studies of the 3% γ-GPS solution (Fig. 5) are similar to previous results [30–32]. The γ-GPS molecule rapidly hydrolyses at a pH of 4.5 and there is no evidence of the condensation reaction leading to siloxane formation. The RAIR spectrum of the γ-GPS film deposited on the ultramilled aluminium surface (Fig. 6) is also typical of previous studies [24–28] and provides some evidence for the condensation of the silanol groups on the aluminium surface leading to the formation of siloxane bonds. The data in Table 3 is consistent with cross-linking of the γ-GPS film. The measured oxygen ratio is lower than would be predicted for the fully hydrolysed γ-GPS molecule and may also suggest the formation of siloxane and Al–O–Si bonds. Time-of-flight secondary ion mass spectrometry (ToF-SIMS) studies [33,34] of silane films deposited on grit-blasted aluminium have provided evidence of siloxane formation as well as Al–O–Si covalent bond formation between the γ-GPS molecule and surface aluminium hydroxyl groups. Previous work [5] has also indicated that the γ-GPS molecule inhibits oxide growth, relative to untreated aluminium surfaces, in humid environments, which also provides support for the conclusion that covalent bonds form between the γ-GPS and aluminium oxide surface.

The data in Table 2 also indicate the presence of contaminant in the γ-GPS film. The ratio of peaks at 285.0 eV, saturated hydrocarbon [19] and 286.5 eV, carbon in alcohol or ether functional groups [19], is 0.82, compared with 0.5 predicted from the γ-GPS chemical structure. This ratio suggests that hydrocarbon contaminant is present in the film. The composition of the surface contaminant present on the ultramilled aluminium surface also appears to alter after γ-GPS treatment (Fig. 3). The component at 289.4 eV, typically assigned to carbon in functional groups similar to carboxylic acids [19], reduces. This may suggest that in some locations the γ-GPS displaces the surface contaminant on the aluminium surface. This process would

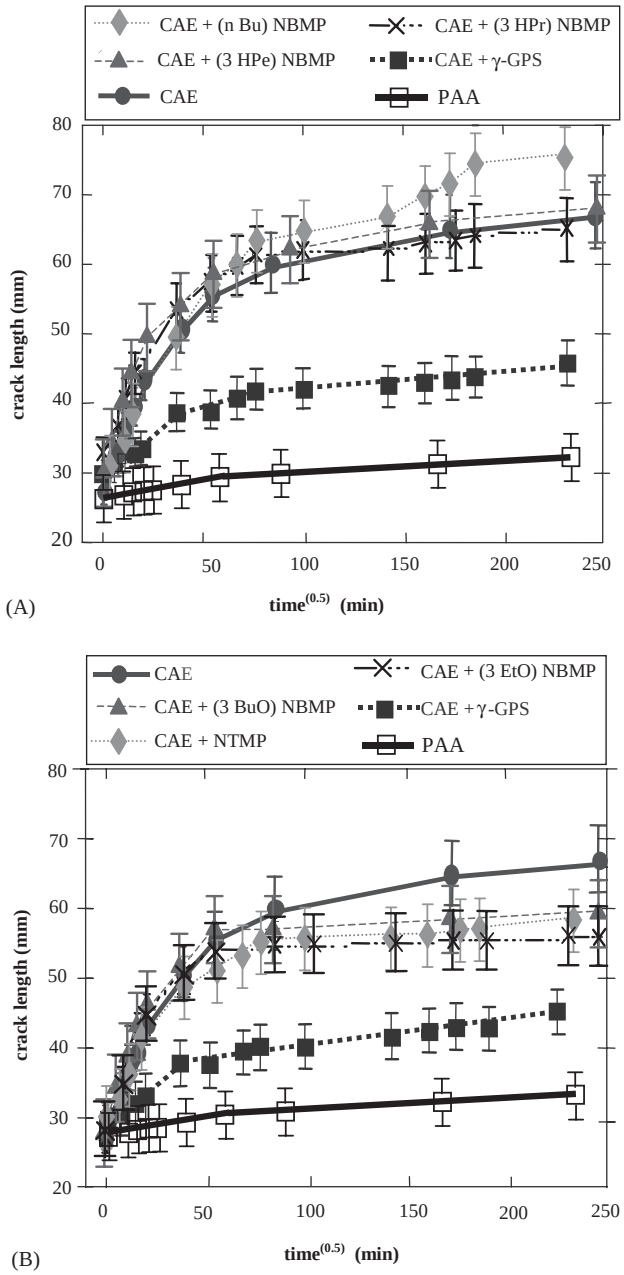

Fig. 8. Wedge test data indicating the durability of Al-2024 T3 clad aluminium (A) chromic acid etched (CAE) and (B) CAE and treated with γ-GPS or phosphonate prior to bonding with FM-73 adhesive.

be necessary for the formation of Al–O–Si bonds implied by the ToF-SIMS studies [34] and for the hydration inhibiting properties of the γ-GPS film [5]. The film thickness of 1.9 nm (Fig. 4) for the γ-GPS-treated aluminium is greater than would be expected for monolayer coverage, given molecular dynamics simulations [35] suggests that the length of the γ-GPS molecule is 1.3 nm. The thickness value may indicate that the film comprises of regions where more than one layer of γ-GPS has adsorbed, with the XPS and RAIR data suggesting that the molecules may be bonded through siloxane linkages. The presence of carbon contaminant in the γ-GPS film will also contribute to the film thickness and coverage measurement established from the ARXPS experiments and prevents definitive conclusions being made about the film properties.

The calculated and measured stoichiometric ratio of the phosphonate films on the ultramilled aluminium surface (Table 3) all indicates oxygen levels below those expected. As with the γ-GPS film, this may provide evidence of bond formation between the phosphonate head group and the surface aluminium hydroxyl groups. The formation of ionic bonds between the ionised phosphate groups and aluminium hydroxyl groups involves water displacement [12] and was confirmed with spectroscopic studies [36]. The ratio of C1s peak components at 285.0 eV, due to saturated hydrocarbon, and 286.0–286.5 eV, due to C-O and C–N bonding [19], in the phosphonate films (Table 2), however, is higher than would be predicted from the phosphonate molecular structure. This suggests, as with the γ-GPS film, that there is carbon contaminant present in the phosphonate films. The reduction in the peak at 289.5 eV, seen in the ultramilled C1s spectrum (Table 2) after phosphonate treatment, suggests that, as with the γ-GPS treatment, displacement of some carbon contaminant has enabled bond formation between the aluminium hydroxyl surface groups and the phosphonate to proceed. The inhibition of oxide hydration measured for the phosphonate-treated aluminium [5] and spectroscopic evidence [36] would be consistent with this mechanism.

Film thickness measurements of the phosphonate-treated aluminium are similar to the values expected, based on simple calculations using bond length data [37], apart from the NTMP film. The NTMP molecule would be expected to be approximately 0.5 nm in length and the film thickness is almost three times this value (Fig. 4). This may indicate multi-layer phosphonate absorption in some regions of the film. The film thickness measurements for the other phosphonate treatments may suggest that single molecule absorption has occurred in regions where the phosphonate is bonded to the aluminium. Carbon contamination present in the films will also contribute to film thickness and coverage measurements made using ARXPS, preventing definitive conclusions regarding the phosphonate film structure being established.

4.2. Adhesion durability and failure surface analysis

The durability data in Fig. 7 suggests that addition of the γ-GPS to the ultramilled aluminium surface improves bond durability. Durability, however, is also influenced by the surface roughness of the aluminium adherend. The fracture surface analysis of the failed wedge test samples (Table 4) suggests that the

Table 5
Elemental compositions of the fracture surfaces resulting from failed wedge test samples pretreated with CAE and γ-GPS or phosphonate solutions

Aluminium pre-treatment	Failure surface	Atomic concentration (%)				
		A12p	C1s	P2p	O1s	Si2p
CAE	Adhesive	3.1	77.9	—	19.0	—
	Metal	22.0	23.2	—	54.8	—
CAE + γ-GPS	Adhesive	4.2	68.8	—	25.0	2.0
	Metal	18.5	39.2	—	41.2	1.1
CAE + NTMP	Adhesive	2.8	72.2	1.1	23.9	—
	Metal	25.2	27.8	2.2	44.8	—
CAE + (3Bu)NBMP	Adhesive	5.1	72.9	2.8	19.2	—
	Metal	17.5	37.5	0.9	44.1	—
CAE + (3HPr)NBMP	Adhesive	1.8	74.5	2.2	21.5	—
	Metal	25.5	30.2	1.8	42.5	—
CAE + (3HPe)NBMP	Adhesive	3.3	75.9	2.1	18.7	—
	Metal	18.2	44.9	1.1	35.8	—
CAE + (3EtO)NBMP	Adhesive	2.2	74.2	1.8	21.8	—
	Metal	15.3	39.3	2.7	42.7	—
CAE + (3BuO)NMBP	Adhesive	3.5	76.3	1.7	18.5	—
	Metal	17.2	46.5	2.8	33.5	—

displacement of adhesive bonds by moisture, that is present at the epoxy–aluminium interface, is the main process that leads to the degradation in bond durability. In the case of untreated ultramilled aluminium, the improvement afforded by increasing the surface roughness may be due to a combination of effects. These effects may include an increase in adherend surface area, thereby increasing the number of interfacial bonds, increases in energy dissipation processes in the adhesive caused by high stress concentrations at surface asperities [38,39] or increases in the interfacial path length for moisture diffusion. If moisture diffusion along the interface was the main process leading to adhesive bond displacement, then the increase in path length for diffusion from the flat 180° to the 60° ultramilled sample may contribute to the improved adhesive bond durability. In relative terms, the path length at the interface would be 1 for the 180° sample, approximately 1.4 for the grit-blast sample and 2.0 for the 60° ultramilled sample. Whilst the path length for interfacial diffusion increases twofold in going from a flat to a 60° ultramilled surface, the change in fracture energy, that could be estimated from the final crack-length values using fracture mechanics [12], would suggest that there is an order of magnitude difference in performance between the two samples. This may suggest that the mechanisms leading to bond degradation are more complex than can be explained by the effect of path-length on interfacial moisture diffusion. The addition of the γ-GPS to the aluminium surface may improve the bond durability by increasing the hydrolytic stability of the interfacial bonds.

Fig. 8 indicates that the bond durability of the phosphonate treatments is inferior to the γ-GPS treatment. The γ-GPS and phosphonate-treated CAE-treated aluminium wedge specimens also degrade as a result of moisture degrading bonds at the epoxy–aluminium interface (Table 5). These results suggest that the bonds formed between the adhesive and aluminium, that was treated with phosphonate, are not as hydrolytically stable as the bonds formed between the adhesive and aluminium, that was treated with γ-GPS. Previous work has indicated the importance of the organic ligand present on the silane molecule that couples with the epoxy adhesive on bond strength and durability [40–42]. Both the chemical make-up and length of the organic ligand appear to be important in the formation of a covalent bond between the adhesive and silane coupling agent. The range of organic ligands, tested using the phosphonate molecule, confirm the importance of this reaction. The data in Fig. 8 suggest that the saturated hydrocarbon chain and the alcohol-terminated alkane chains do not improve the hydrolytic stability of interfacial bonds. The NTMP molecule and the phosphonates with alkoxy-based ligands, that more closely resembled the γ-GPS chemistry, showed improved durability, suggesting improvement of the hydrolytic stability of the organic ligand to adhesive bond.

The phosphonate molecules tested, however, did not have an organic ligand identical to that present on the γ-GPS and this may be one of the important reasons for the relative durability performance of the γ-GPS and phosphonate treatments. A phosphonate molecule with an epoxy ligand could not be tested due to difficulty in synthesising the compound with the method described (Section 2.1).

Hydration studies suggest that the hydrolytic stability of the Al–O–P bond, resulting from phosphonate

treatment of aluminium, is greater than the Al–O–Si bond produced for the γ-GPS treatment [5]. This difference in hydrolytic stability may suggest that other factors also contribute to the bond durability performance of the γ-GPS treatment. The presence of silicon and phosphorous on both fracture faces of the failed wedge samples (Table 5) indicates that the structure of the γ-GPS and phosphorous films may also influence bond durability. There is some evidence (Section 4.1) that the γ-GPS film on the aluminium surface is strengthened cohesively through siloxane bonds. A number of research papers have also indicated that the use of the silane cross-linking agent bis-trimethoxy silylethane, $(MeO)_3SiC_2H_4Si(OMe)_3$, can improve bond durability [43–45], which also provides an indication that the cohesive strength of the silane film may influence bond durability. ToF-SIMS studies [33] have also indicated that the cross-linking of the γ-GPS film increases when it is heated above 90 °C. Bond durability improvement is also observed with this heat treatment [10]. The absence of a similar cross-linking mechanism in the phosphonate film layer [46,47] may make a contribution to the poorer durability performance in the wedge durability tests.

Future experiments that could further investigate the effect of film cross-linking and interaction between the organic ligand and the epoxy resin may involve synthesis of a phosphonate molecule with an epoxy ligand and investigation of mono- and di-alkoxy silane molecules.

5. Conclusions

Film characterisation studies of ultramilled aluminium treated with γ-GPS indicate that the film is thicker than would be expected for monolayer adsorption and contains hydrocarbon-based contaminant. There is also some evidence that the film is cohesively bonded through siloxane linkages.

Phosphonate-treated ultramilled aluminium indicates that, apart from the NTMP, the film thickness values are similar to those expected for monolayer adsorption. The NTMP-treated aluminium suggests that film regions exist where multiple layer adsorption may have occurred. As with the γ-GPS treatment, there is evidence that the films contain regions of hydrocarbon-based contaminant.

Increasing the surface roughness of the aluminium adherend, using either grit-blasting or milling blades with increasing profile angles, improved the bond durability performance of wedge test specimens. Additional treatment of the grit-blasted or ultramilled surfaces with γ-GPS further improved the durability of wedge test specimens. The overall bond durability performance of the γ-GPS-treated samples, however, was influenced by the adherend surface roughness, with the flat sample showing inferior durability to both the grit-blasted and the ultramilled sample with a 60° profile angle.

An important factor that influenced bond durability was the chemistry of the organic ligand on the phosphonate molecule that interacted with the epoxy adhesive. When the organic ligand on the phosphonate molecule improved the durability of the CAE treatment, the performance was still inferior to the CAE and γ-GPS treatment.

Fracture analysis of failed wedge test specimens suggested that the presence of moisture at the adhesive–aluminium interface resulted in water displacing adhesive bonds that then led to bond degradation. The presence of silicon and phosphorous on the complementary fracture faces suggested that the cohesive strength of the phosphonate or γ-GPS film is one property that could potentially contribute to bond durability performance. The absence of primary chemical bonds linking the phosphonate film may contribute to the poorer performance in wedge style adhesive bond durability tests.

Acknowledgement

The author would like to thank Dr. Naresh Kumar at UNSW Chemistry Department for synthesis of the phosphonate compounds used in this work.

References

[1] Baker AA, Chester RJ. Int J Adhes Adhes 1992;12:73.
[2] Farr NG, Arnott DR, Rider AN, Griesser HJ. In: The Australian Aerospace Conference, Melbourne, 9–11 October 1989, Preprints of Papers, p. 216–220, Institute of Engineers, Australia, 1989 (ISBN 0-85825-48 1-6).
[3] Arnott DR, Rider AN, Wilson AR, Lambrianidis LT, Farr NG. In: International Conference on Aircraft Damage Assessment and Repair, Melbourne. 1991, p. 149.
[4] Olsson-Jacques CL, Wilson AR, Rider AN, Arnott DR. Surf Interface Anal 1996;24:569.
[5] Rider AN, Arnott DR. Surf Interface Anal 1996;24:583.
[6] Arnott DR, Rider AN, Olsson Jacques CL, Lambrianidis LT, Wilson AR, Pearce PJ, Chester RJ, Baker AA, Morris CEM, Davis MJ, Swan G. In: Proceedings of 21st Congress ICAAS, Melbourne. 1998.
[7] Rider AN, Arnott DR. Int J Adhes Adhes 2000;20:209.
[8] Royal Australian Air Force Engineering Standard C5033, Composite Materials and Adhesive Bonded Repairs, RAAF Headquarters Logistics Command, Melbourne. 1995.
[9] Davis MJ. In: Proceedings of 41st International SAMPE Symposium. 1996, p. 936.
[10] Kuhbander RJ, Mazza JP. In: Proceedings of 38th International SAMPE Symposium, vol. 38. 1993, p. 1225.
[11] Digby RP, Shaw SJ. Int J Adhes Adhes 1998;18:261.
[12] Venables JD. J Mater Sci 1984;19:2431.
[13] Rider AN. PhD thesis, University of New South Wales, 1998.
[14] Rider AN, Olsson-Jacques CL, Arnott DR. Surf Interface Anal 1999;27:1055.

[15] Morawietz H, Hoffmann E, Hanauer J, Bauer K, German Patent DE 3128755A1, 1983.
[16] ASTM. Annual book of ASTM Standards. Section 15, vol. 15.06, Adhesives. Philadelphia: ASTM; 1992.
[17] Lambrianidis LT, Arnott DR, Wilson AR, Van den Berg J, Vargas O. In: Proceedings of International Aerospace Congress, Melbourne. 1995, p. 355.
[18] Marceau JA. In: Thrall EW, Shannon RW, editors. Adhesive bonding of aluminium alloys. New York: Marcell-Dekker; 1985 [Chapter 4].
[19] Beamson G, Briggs D. High resolution XPS of organic polymers. Chichester: Wiley; 1992.
[20] Arnott DR, Wilson AR, Rider AN, Lambrianidis LT, Farr NG. Appl Surf Sci 1993;70:109.
[21] Fadley CS. In: Davison SG, editor. Progress in surface science. New York: Pergamom; 1985.
[22] Tanuma S, Powell CJ, Penn DR. Surf Interface Anal 1988;11:577.
[23] Peters GR, Luoma GA. DREP technical memorandum 89-24, 1989.
[24] Underhill PR, Goring G, DuQuesnay DL. Appl Surf Sci 1998;134:247.
[25] Underhill PR, Goring G, DuQuesnay DL. Int J Adhes Adhes 2000;20:195.
[26] Culler SR, Ishida H, Koenig JL. J Coll Interface Sci 1986;109:1.
[27] Naviroj J, Koenig L, Ishida H. J Adhes 1985;18:93.
[28] Ondrus DJ, Boerio FJ. J Coll Interface Sci 1988;124:349.
[29] Digby RP, Porritt N, Shaw SJ, Watts JF. In: Proceedings of Adhesion Society 23rd annual meeting (USA). 2000, p. 473.
[30] Pohl ER, Osterholtz FD. In: Mittal KL, editor. Silanes and other coupling agents. Utrecht: VSP; 1992. p. 119–41.
[31] Pohl ER, Osterholtz FD. In: Ishida H, Kumar G, editors. Molecular characterisation of composite interfaces. New York: Plenum; 1985. p. 157–70.
[32] Bertelsen CM, Boerio FJ. J Adhes 1999;70:259.
[33] Abel M-L, Acharawan R, Watts JF. J Adhes 2000;73:313.
[34] Abel M-L, Digby RP, Fletcher IW, Watts JF. Surf Interface Anal 2000;29:115.
[35] Davis SJ, Watts JF. Int J Adhes Adhes 1996;16:5.
[36] Henricksen PN, Gent AN, Ramsier RD, Alexander JD. Surf Interface Anal 1988;11:283.
[37] Lide DR. CRC handbook of chemistry and physics, 76th ed. New York: CRC Press; 1995 [p. 9–1].
[38] Evans JRG, Packham DE. J Adhes 1979;10:177.
[39] Packham DE. Int J Adhes Adhes 1986;6:225.
[40] Thiedman W, Tolan FC, Pearce PJ, Morris CEM. J Adhes 1987;22:197.
[41] Abel M-L, Acharawan R, Watts JF. Langmuir 2000;16:6510.
[42] Harding PH, Berg JC. J Appl Polym Sci 1998;67:1025.
[43] Plueddemann EP. J Adhes Sci Technol 1988;2:179.
[44] Child TF, van Ooij WJ. Trans Inst Metal Finishing 1999;77:64.
[45] Adams AN, Kinloch AJ, Digby RP, Shaw SJ. In: Proceedings of EURADH'2000—fifth European Adhesion Conference, Lyon. 2000, p. 320.
[46] Davis GD, Shaffer DK, Matienzo LJ, Ahearn JS. J Vac Sci Technol A 1985;3:1418.
[47] Ahearn JS, Davis GD. J Adhes 1989;28:75.